Mon. Not. R. Astron. Soc. **299,** 643–652 (1998)

Triggered star formation in the LMC4/Constellation III region of the Large Magellanic Cloud

Yuri N. Efremov[1] and Bruce G. Elmegreen[2⋆]
[1]*MSU, P.K. Sternberg Astronomical Institute, Moscow 119899, Russia*
[2]*IBM Research Division, T.J. Watson Research Center, PO Box 218, Yorktown Heights, NY 10598, USA*

Accepted 1998 April 1. Received 1998 March 20; in original form 1997 July 10

ABSTRACT

The origin of a regular, 600-pc-long arc of young stars and clusters in the Constellation III region of the Large Magellanic Cloud is considered. The circular form of this arc suggests that the pre-stellar gas was uniformly swept up by a central source of pressure. In the centre of the arc are six ∼30-Myr-old A-type supergiant stars and a Cepheid variable of similar age, which may be related to the source of this pressure. We calculate the expansion of a bubble around a cluster of this age, and show that it could have triggered the formation of the arc at the right time and place. Surrounding the central old stars and extending well outside the young arc is the LMC4 superbubble and giant H I shell. We show how this superbubble and shell could have formed by the continued expansion of the 15-Myr-old cavity, following star formation in the arc and the associated new pressures. The age sequence proposed here was not evident in the recent observations by Olsen et al. and Braun et al. because the first generation stars in the centre of the LMC superbubble are relatively faint and scarce compared to the more substantial population of stars less than 15 Myr old that formed throughout the region in a second generation. These considerations lead to an examination of the origin of the LMC4/ Constellation III region and other large rings in the LMC and other galaxies. Their size and circularity could be the result of low galactic shear and a thick disc, with several generations of star formation in their interiors now too faint to be seen.

Key words: instabilities – stars: formation – ISM: bubbles – Magellanic Clouds.

1 INTRODUCTION

Two large arcs of young stars and clusters are prominently situated in the north-east corner of the Large Magellanic Cloud (LMC) (see Fig. 1). One is large and thick, being a quarter segment of a ring (designated the 'Quadrant' here), and usually identified with Shapley's Constellation III. The other, slightly to the south-west, is smaller and contains brighter clusters shaped like one-sixth part of a ring ('Sextant'). The Quadrant consists of Lucke & Hodge (1970) associations LH 65, 77 and 84, and is often referred to as LH 77; the Sextant includes LH 51, 54, 60 and 63, and is not generally considered noteworthy, being often masked by bright H II regions (cf. Table 1). The main peculiarity of both arcs is their very regular circular form.

The region surrounding these arcs is well studied as a possible example of propagating star formation. Westerlund & Mathewson (1966) noted on a UV plate 'the great arc of the bright blue stars', saying that 'Shapley called this arc Constellation III'; they also suggested this arc is connected with the supergiant H I shell that surrounds the most prominent H I void in the LMC, noted by McGee & Milton (1966). The inner extent of this shell, as determined by Kim et al. (1997), is shown in Fig. 1 by a circle.

Westerlund & Mathewson (1996) further suggested that 'the annular shell of neutral hydrogen and stars in the region of Constellation III' is the remnant of a 'super-supernova' outburst (following Shklovsky 1960). They believed that gas was swept up by the expanding shell; the part of this shell that was moving to the centre of the LMC would accumulate matter more quickly and be the first to become stationary. Stars would condense out, forming the arc of stars of Constellation III. They believed also that the southern part of the H I supershell is missing, and that 'this gap is filled by the arc of bright blue stars forming Constellation III'. This latter suggestion is not confirmed by the H I data, which show the southern part of the H I shell clearly (Domgörgen, Bomans & de Boer 1995; Kim et al. 1997).

The enormous elongated ring of H II regions around the H I void, designated superbubble LMC4, was found later by Meaburn (1980). The H I void, the surrounding H I shell, and the H II regions and clusters of the superbubble LMC4 were all considered by Dopita, Mathewson & Ford (1985) to be the result of supernovae and O-type stars near the centre of LMC4. They believed they saw an age gradient, and determined the velocity of the star formation front,

⋆ E-mail: bge@watson.ibm.com

propagating outward from the centre, to be 36 km s^{-1}, which was the same as the velocity of the H I shell that they measured. Subsequent investigations have not confirmed the age progression or H I velocity (Reid, Mould & Thompson 1987; Domgörgen et al. 1995; Braun et al. 1997; Olsen et al. 1997), although many still believe that LMC4 and the ring of young clusters is connected with triggered star formation. Olsen et al. found that the age of LH 72, which is near the centre of Constellation III, is about the same as the ages of the young clusters along the LMC4 ring, although the age spread in LH 72 is large, with stars ranging between 5×10^6 and 1.5×10^7 yr old. Olsen et al. concluded that their data are consistent with the alternative model by Reid et al. (1987), in which star formation proceeded locally for a long time after an initial trigger from the LMC4 superbubble shock. Braun et al. found no signs of an age gradient in the region, obtaining ages of field stars within a J-shaped strip inside LMC4, including Quadrant but not LH 72.

Domgörgen et al. (1995) studied the origin of the superbubble. They considered stellar winds and supernovae in the central association, the collision of a high-velocity cloud with the LMC disc, and the large-scale propagation of star formation, concluding that the latter process is more probable.

There is a third, larger, arc to the south of Quadrant, open to the north-east and touching Quadrant at the north-west. It is rather dispersed, and the age spread along it is large, but at the centre of curvature of this arc there is a massive cluster, NGC 2041, that is older than most of the clusters within the arc. Members of this arc are listed in Table 1. It may be another example of triggered star formation, but it is less well defined than Quadrant and Sextant, so we do not discuss it further. All three arcs were noted and sketched by Hodge (1967), who also found similar features in NGC 6946.

Here we consider the possibility that the Quadrant and Sextant arcs formed by instabilities in a swept-up ring and shell respectively. We also show how the giant H I ring surrounding Quadrant could have been rejuvenated by new pressures from these stars after the first generation pressures subsided. We then discuss why the LMC4 region appears so unusual compared to shells and rings in other galaxies. We do not comment on the origin of the first generation of stars (see, e.g., de Boer et al. 1998), but only point out some likely members based on catalogues of supergiants and Cepheid variables.

2 STAR CLUSTER ARCS

We first consider the nomenclature of features in this region. Shapley's original name of Constellation III was given to another region, not to what is commonly considered to be Constellation III.

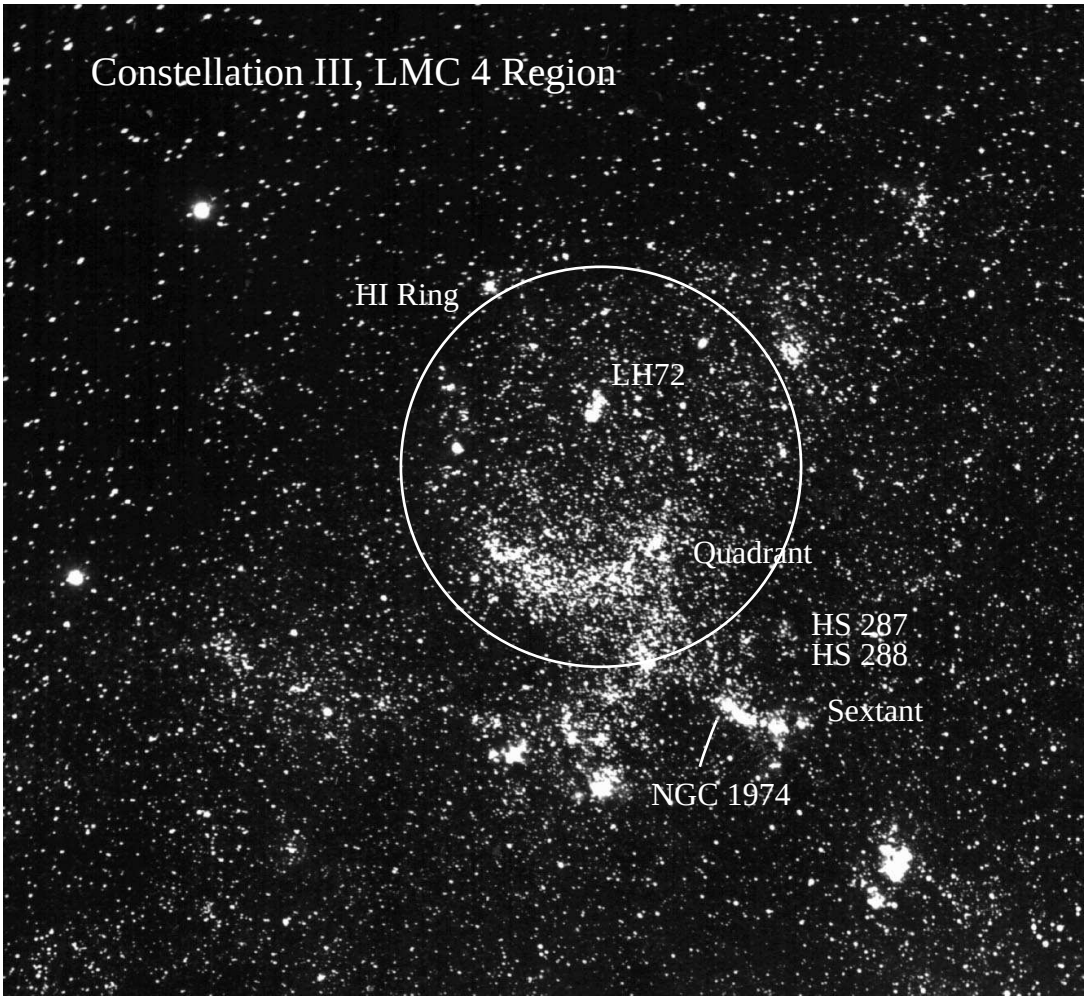

Figure 1. Photographic image of the Constellation III region of the LMC, with a circle indicating the inner radius of the H I shell and other identifications discussed in the text. The diameter of the circle is 1.32 deg. The original photograph is from Boyden Observatory, courtesy of Harlow Shapley, Harvard College Observatory, and kindly provided in tiff form by Knut Olsen, Paul Hodge and Don Brownlee.

Table 1. Clusters within arcs.

Arc	Cluster	V	$U-B$	$B-V$	X (°)	Y (°)	S	$\log t$
Quadrant								
	KMK987	12.32	−0.73	−0.12	−0.91	2.59	15	7.33
	NGC2002 = SL517	10.10	−0.58	0.34	−0.89	2.61	13	7.18
	SL538	11.30	−0.67	−0.01	−0.98	2.53	15	7.33
	NGC2006 = SL537	10.88	−0.63	0.12	−0.98	2.52	15	7.33
	KMK1019	11.49	−0.57	0.48	−1.03	2.49	12	7.11
	LH 77p1	10.55	−0.64	0.19	−0.97	2.47	13	7.18
	LH 77p2	10.09	−0.65	0.10	−1.26	2.49	14	7.25
	LH 77p3	10.39	−0.73	0.04	−1.09	2.51	13	7.18
	NGC2027 = SL592	10.97	−0.89	0.000	−1.34	2.58	8	6.82
	KMK1074	12.61	−0.80	−0.15	−1.24	2.49	13	7.18
	SL586 = ESO86sc12	11.17	−0.80	−0.12	−1.31	2.53	13	7.18
	NGC2034n	9.78	−0.58	0.29	−1.41	2.62	14	7.25
	NGC2034s	10.35	−0.75	0.24	−1.39	2.58	9	6.89
Sextant								
	SL456 = LH 51	11.75	−1.02	−0.23	−0.41	2.01	7	6.74
	NGC1955 = LH 54	9.83	−1.00	−0.21	−0.46	1.99	7	6.74
	NGC1968w = LH 60w	10.78	−0.96	−0.04	−0.62	2.03	5	6.60
	NGC1968e = LH 60e	10.20	−1.06	−0.21	−0.60	2.03	4	6.52
	NGC1974 = LH 63	10.30	−0.97	−0.21	−0.65	2.06	8	6.82
Center	HS 288				−0.55	2.25		
	HS 287				−0.48	2.35		
Third Arc								
	Inside N59:							
	NGC2040 in LH 82	11.47	−0.95	−0.18	−1.42	1.93	9	6.89
	NGC2035 in LH 82	10.99	−0.76	−0.17	−1.37	1.91	15	7.33
	NGC2032 in LH 82	10.80	−0.58	−0.19	−1.35	1.93	19	7.62
	NGC2029 in LH 82	12.29	−0.68	−0.39	−1.32	1.94	19	7.62
	Inside N56:							
	NGC2021 in LH 79	12.06	−0.77	−0.13	−1.18	2.04	14	7.25
	SL567 in LH 78	10.19	−0.83	0.09	−1.15	1.97	9	6.89
	NGC2011 in LH 75	10.58	−0.71	0.04	−1.06	1.98	13	7.18
	NGC2004	9.60	−0.71	0.13	−0.91	2.20	12	7.11
	SL522	12.10	−0.78	−0.09	−0.91	2.30	13	7.18
	SL516	12.14	−0.61	−0.05	−0.85	2.51	17	7.47
	NGC2002 = SL517	10.10	−0.58	0.34	−0.89	2.61	13	7.18
Center	NGC2041	10.36	−0.17	0.22	−1.48	2.51	24	7.99

McKibben Nail & Shapley (1953) designated NGC 1974 as the identifier of Constellation III, including an area of 28×28 arcmin^2 around NGC 1974 (see Fig. 1). They also noted that Constellation III is a triple cluster, so in fact they were probably referring to Sextant. This is sensible because Sextant is brighter than Quadrant (cf. Fig. 1), and would have been more noticeable to McKibben Nail & Shapley. Map V45 in the Hodge & Wright (1967) Atlas of the LMC clearly shows that NGC 1974 is within Sextant, and what is commonly called Constellation III, which is the large arc called Quadrant by us, is not within the 28×28 arcmin^2 field around NGC 1974.

Westerlund & Mathewson (1966) were evidently the first to identify 'the arc of bright blue stars' (i.e., Quadrant) with Shapley's Constellation III. Olsen et al. (1997) also called Quadrant Constellation III in their fig. 1, yet in the text they refer to the entire superbubble LMC4 as Constellation III. Van den Bergh (1981) called the whole LMC4 region Constellation III as well. This identification was typically the case in papers concerning the whole region, and was probably one of the reasons why neither Quadrant nor Sextant has been considered as a peculiar feature deserving study by itself.

The Quadrant and Sextant arcs are indeed unique features; there is nothing similar in the LMC. Quadrant consists of both clusters and individual stars, and may also be designated as LH 77 (the small associations LH 84 and 65 are inside of it). Sextant includes LH 51 = SL 456, LH 54 = NGC 1955, LH 60 = NGC 1968 and LH 63 = NGC 1974 (Lucke & Hodge 1970, fig. 1 and table 1; NGC 1974 is misprinted as NGC 1947 in their table).

Similar arcs of star clusters have not been reported elsewhere either. Besides the NGC 6946 features (Hodge 1967), the only thing resembling the Quadrant and Sextant stellar arcs is a large region in the galaxy NGC 1620 studied by Vader & Chaboyer (1995). At the inclination of this galaxy, it is difficult to tell if this is a triggered arc or a spiral arm.

Data on all three arcs are given in Table 1. The integral *UBV* and position data were taken from Bica et al. (1996), and the ages were determined from the $U-B$ and $B-V$ data via the S values according to Girardi et al. (1995). Girardi et al. introduced S values as a combination of $U-B$ and $B-V$ integral colours of clusters, and calibrated these values as a function of age, using 24 rich clusters with ages determined from colour–magnitude diagrams (CMDs). These clusters gave the $S-\log t$ relation with an rms dispersion of 0.137 in $\log t$ (Girardi et al. 1995). For less populous clusters, the error should be larger.

Only integral colours are available for the bulk of clusters considered here. After this paper was submitted, the preprint by

Braun et al. (1997) became available. It contains age determinations from CMDs of several fields inside LMC4. Fields 0–10 of Braun et al. are within the Quadrant, and their age range is 9–16 Myr (most are within the range 10–14 Myr). The S values for these clusters give an age range within Quadrant (Table 1) that is similar, 7–21 Myr (most are within 10–18 Myr). More detailed comparisons for the Quadrant region are impossible, because the Braun et al. fields are much larger than the clusters measured by Bica et al. (1996). For the Sextant region there are ages obtained by Petr (1994), as given by Braun et al. (in Myr): LH 63 – 14, LH 60 – 9, and LH 54 – 6, whereas our values (Table 1) are respectively 7, 3–4 and 3 Myr. Braun et al. comment that the accuracy of their ages is ∼0.1 in logarithmic units and, because of the different isochrones used, their ages should be slightly older (by 0.05 in $\log t$) than those determined by Girardi et al. (1995). We conclude that ages derived from the integral photometry are consistent with those from the CMDs, and are accurate enough for our purposes.

A remarkable feature of the two arcs is their circularity. This regular form suggests they were produced from nearly uniform gas swept up by a central source of pressure. The smaller size and lower age of Sextant, and its position near the edge of LMC4, suggest that it was triggered inside the dense H I shell that was swept up earlier to make Quadrant.

3 POSSIBLE PRESSURE SOURCES

The radius of the Sextant arc is ∼170 pc, and at its centre there is the small cluster HS 288 (cf. Fig. 1). At 70 pc to the north there is a larger, dispersed cluster, HS 287, surrounded by the H II region N50. For the Quadrant arc the radius is ∼280 pc and there is nothing obvious at the exact centre, but at ∼160 pc to the NNW from the centre of curvature there is a bright cluster LH 72 with an age range of 5–15 Myr (Olsen et al. 1997) surrounded by the H II region N55. These sizes assume a distance to the LMC of 45 kpc (Berdnikov, Vozyakova & Dambis 1996; Efremov 1997; Efremov, Schilbach & Zinnecker 1997; Fernley et al. 1998).

The radius of the Quadrant arc is too large, and the projected expansion speed of the H I shell too small (< 10 km s^{-1}; Domgörgen et al. 1995), for a young cluster like LH 72 to have formed it. Besides, the LH 72 cloud in Kim et al. (1997) looks like a bright rim that is part of a shell coming off from the north-east rim of the LMC4 superbubble, so it is not related to the trigger for Quadrant or the expansion of LMC4.

Sextant is somewhat different: the arc is small and the local density is high, so the formation time could have been much shorter than for Quadrant. There are no age data for the two clusters HS 287 and 288 near the centre of Sextant, but HS 287 must contain at least some young stars, with ages of 10^7 yr or less, considering the ionization in the associated nebula N50. There is also ionization in Sextant, forming a shell around its eastern end, which is N51D (Meaburn & Terret 1980). This is consistent with both its lower age and the higher density of ambient H I compared to Quadrant.

Thus we consider the possibility that the clusters HS 287 and/or HS 288 formed the Sextant arc in only 10 Myr or so, and that older, fainter stars near the centre of curvature of the Quadrant arc formed this larger region.

There are indeed old stars near the centre of the Quadrant arc. At the centre of the LMC4 supershell there is a sparse, faint cluster, HS 343, for which no photometry exists. HS 343 could be much older than LMC4, in which case it would be irrelevant here. (HS 343 is not visible in Fig. 1, so its position is indicated in Fig. 2.)

More important is a small grouping of six A-type supergiant stars

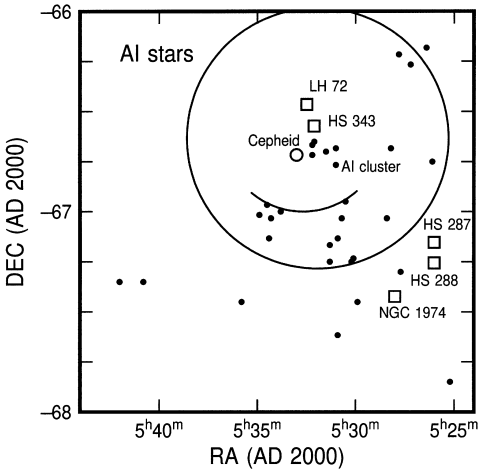

Figure 2. A-type supergiant stars in the vicinity of Constellation III, from the catalogue of Rousseau et al. (1978). The open circle is the Cepheid variable star HV 5924, and the open squares are some of the clusters discussed in the text.

Table 2. A-type supergiant stars near the centre of the LMC4 supershell.

Star	RA (2000.0)	Dec. (2000.0)	V	Sp.T.
NS 119A-66	5h 31m	−66° 46′	12.16	A0 I
NS 120-66	5h 31m	−66° 41′	12.50	A0 I
NS 124-66	5h 31.5m	−66° 42′	12.46	A1 I
G 359	5h 32.1m	−66° 39′	12.51	A9 I
NS 129-66	5h 32.2m	−66° 43′	12.16	A0 I
NS 130-66	5h 32.2m	−66° 40′	12.05	A0 I

in the catalogueue of Rousseau et al. (1978) within a circle of ∼10 arcmin diameter near the centre of curvature of Quadrant. These stars have apparent V magnitudes of 12.1 to 12.5, as given in Table 2. This is the only concentration of type AI or later supergiants within the LMC4 area, as is evident from Fig. 2, which shows all of the A-type supergiants in the region. There are also several B- and M-type supergiants near the centre of LMC4, from the catalogues of Rousseau et al. (1978) and Rebeirot et al. (1983) respectively, but these stars show no particular concentration like that of the A stars.

Isochrones by Bertelli et al. (1994) (the same as those used for the cluster ages here and in Girardi et al. 1995) give $\log t = 7.4$ for AI stars, 7.5 for BI stars and about 7.6 (V magnitudes are uncertain) for MI stars. The positions of these LMC4 supergiants in a CMD are very similar to the positions of the brightest stars in two LMC young globulars, NGC 2004 and 2100. These clusters were used by Girardi et al. to calibrate integral colours as ages. The average ages of the clusters from their CMDs are $\log t = 7.33$ and 7.40, whereas their ages from the blue supergiants are $\log t = 7.66$ and 7.71. The difference is explained by much lower ages for the main-sequence turn-off points, 6.99 and 7.10 respectively. This difference illustrates the age range for star formation, and the uncertainties present in the theory of supergiants. To be more in accordance with the ages from the integral colours, we prefer the ages that are connected with the supergiants stars, because these contribute most strongly to the integral colours of a cluster. This age is ∼30 My, and clearly larger, by ∼15 Myr, than the ages of most of the Quadrant stars.

A Cepheid star, HV 5924, with a period 16.2 d, is close to HS 343 and the AI supergiants; its position is shown in Fig. 2 by an open circle. This period corresponds to an age of 75 Myr, according to a recent calibration in Efremov & Elmegreen (1998). Two other

Cepheids, HV 5921 and 12436, are also nearby, but their periods are much shorter, 3.0 and 4.3 d, and so their ages are greater, 140–180 Myr. Considering the inaccuracy in Cepheid ages, HV 5924 could be coeval with the AI stars, but the other two Cepheids are probably not.

In view of the presence of luminous stars near the centre of LMC4, there must have been significant star-forming activity there about 30 Myr ago. This is presumably the event whose pressures led to the formation of the Quadrant arc, and which also began the current generation of star formation throughout this region. The cluster of six AI stars is not at the exact centre of the Quadrant arc, but this could be the result of a small southerly drift of this cluster from a $\sim$4 km s^{-1} motion of its primordial cloud.

4 TRIGGERED STAR FORMATION IN QUADRANT

4.1 Triggering conditions

We propose that the Quadrant arc of young stellar clusters was formed by the gravitational collapse of swept-up gas in the densest part of an expanding *ring* that surrounded what was then a $\sim$14 Myr-old cluster, but which is visible today as a dispersed group of supergiants and Cepheid variables, $\sim$30 Myr old. The current age of the Quadrant ring is taken to be 16 My, from the oldest stars in this region found by Braun et al. (1997). The total age of $\sim$30 Myr is imprecise. The solutions given below for the triggering and expansion of the Quadrant arc and H I ring depend on this age, but the qualitative nature of the results, i.e., our proposal that stars connected with the cluster of AI supergiants triggered the formation of Quadrant does not depend very much on this total age unless it is wrong by more than a factor of 2.

The ring geometry assumed here is important, as opposed to a three-dimensional shell geometry, because the divergence of gas in a ring differs from the divergence in a shell, giving a different equation for the collapse time (Elmegreen 1994). Rings are also more likely than shells for large disturbances in galaxy discs, because the gravity of the disc pulls high-latitude shell material down to the mid-plane where it makes a ring, and because most of the ambient gas that is compressed by the disturbance is close to the plane (Ehlerová et al. 1997).

The formation of giant molecular clouds in expanding *shells* of gas has been considered a mechanism for triggered star formation since the work of Tenorio-Tagle (1981) and Elmegreen (1982a,b). The first analytical work on gravitational instabilities in expanding shells was by Ostriker & Cowie (1981) and Vishniac (1983). A more detailed analytical analysis of shell expansion and collapse, with applications to triggered star formation in galaxies, was carried out by McCray & Kafatos (1987). The first work on gravitational instabilities in expanding rings was by Elmegreen (1985). The basic idea in these references is the same as that applied here to the Quadrant and Sextant arcs.

In this model, gas that is collected into a compressed ridge by a moving shock front becomes gravitationally unstable because of its high density, and it forms one or more cores with even higher density. Stars form in these high-density cores by normal processes, but at a much higher rate than would have occurred without the compression. This is the triggering model introduced by Elmegreen & Lada (1977). It is distinct from another prominent triggering mechanism in which pre-existing clouds are imploded by a shock front directly. The implosion model dates back to Dibai (1958) and Dyson (1968), with recent work by Lefloch & Lazareff (1994), Boss (1995) and others. It was applied to the Constellation III region by Dopita et al. (1985). The first model, sometimes called the 'collect and collapse' model, is preferred to the implosion model for the Quadrant region, because Quadrant consists of semiregularly spaced clusters with a uniform size strung out along an arc, in addition to many bright field stars. This is precisely the geometry expected for an instability in a swept-up piece of a ring; each cluster formed at a local centre of collapse. Implosion models should give a more irregular placement of second generation regions, as Dopita et al. discussed. A review of both triggering mechanisms is in Elmegreen (1998).

Here we consider two models for a ring expanding into a uniform medium. The first has a shock velocity $V \propto t^{-0.4}$ and radius $R \propto t^{0.6}$ in the case where energy is continuously put into a spherical cavity from combined supernovae and stellar winds (Pikelner 1968; Dyson 1973; Castor, McCray & Weaver 1975; for a more recent discussion, see Comerón, Torra & Gómez 1998). The three-dimensional shape of the cavity may not be this simple, however, because the perpendicular extent may be larger than the in-plane extent (e.g. Tenorio-Tagle & Bodenheimer 1988). An alternative model considers that the energy in a cylinder increases linearly with time, rather than the energy in a sphere. The mass of a cylinder increases as R^2, so the energy constraint in this case gives $R^2V^2 \propto t$ instead of $R^3V^2 \propto t$ for a sphere. The similarity solution for the expansion is then $R \propto t^{3/4}$ and $V \propto t^{-1/4}$. These two cases will be designated as spherical and cylindrical energy input respectively. For a general derivation of the collapse conditions, we write $R \propto t^{\kappa}$, where $\kappa = 3/5$ and 3/4 in the spherical and cylindrical geometries respectively.

The collapse time for a ring with an $R \propto t^{\kappa}$ expansion law may be derived following the example in Elmegreen (1994). The model considers the accumulation and divergence of material in a ring with half-thickness r, compressed density ρ, mass per unit length $\mu_0 = \rho\pi r^2 = \rho_0 Rr$, turbulent velocity dispersion in the ring, c, angular velocity of the growing perturbation, Ω, and pre-shock density $\rho_0 = n_0 m_{\rm H}$. With perturbed quantities indicated by a subscript 1, the equations of motion and continuity for the growth of transverse perturbations are

$$\mu_0 R\frac{\partial\Omega}{\partial t} = -c^2\nabla\mu_1 + \mu_0 g_1 - 3\mu_0\Omega V, \tag{1}$$

$$\frac{\partial\mu_1}{\partial t} = -\mu_0 R\nabla\cdot\Omega - \mu_1\frac{V}{R}. \tag{2}$$

The self-gravitational acceleration $g_1 = 2G\mu_1 k\ln(2/kr)$ is for a perturbation along the periphery of the ring with wavenumber $k = 2\pi/\lambda$ and wavelength λ; this approximation is reasonable for $2 >> kr$.

We consider sinusoidal perturbations and let the time derivatives in the above equations equal the instantaneous growth rate ω. Then Ω and μ_1 can be eliminated, and an equation for ω as a function of k results (see Elmegreen 1994):

$$\omega = -\frac{2V}{R} + \left[\frac{V^2}{R^2} + 2G\mu_0 k^2\ln(2/kr) - c^2k^2\right]^{1/2}. \tag{3}$$

Setting $\mathrm{d}\omega/\mathrm{d}k = 0$ gives the fastest growing wavelength, and after substituting this into the equation for ω we get the fastest growth rate:

$$\omega_{\rm peak} = -\frac{2V}{R} + \left(\frac{V^2}{R^2} + G\mu_0 k_{\rm peak}^2\right)^{1/2}, \tag{4}$$

where

$$\frac{k_{\rm peak}r}{2} = \exp\left[-0.5\left(1 + \frac{c^2}{G\mu_0}\right)\right]. \tag{5}$$

Now we set the fastest growth rate equal to the inverse of the ring age in order to get the time of significant collapse after the beginning of the expansion; for $R \propto t^{\kappa}$, this time is $t = \kappa R/V$ (see also Ehlerová et al. 1997 and Theis et al. 1997). This leads to an equation for t that has to be solved iteratively, since μ_0 in the exponent of equation (5) depends on t, i.e., $\mu_0 = \rho\pi r^2 = \rho_0 \mathcal{M}^2 \pi r^2$ for shock speed V as a function of t; here we have assumed a shock compression of $\rho/\rho_0 = (V/c)^2 \equiv \mathcal{M}^2$. The result is

$$t \exp\left[-0.5\left(1 + \frac{c^2}{G\mu_0}\right)\right] = \frac{[(1+2\kappa)^2 - \kappa^2]^{1/2}}{(4\pi G\rho_0)^{1/2}\mathcal{M}}. \tag{6}$$

To solve this, we write

$$t = \frac{T_0}{(G\rho_0)^{1/2}\mathcal{M}}, \tag{7}$$

and introduce the galactic scaleheight

$$H^2 = \frac{c_0^2(1+\alpha+\beta)}{2\pi G\rho_{0\mathrm{T}}} \quad \text{for} \quad \alpha = \frac{B^2}{8\pi P} \quad \text{and} \quad \beta = \frac{P_{\mathrm{CR}}}{P}, \tag{8}$$

with ambient magnetic field strength B, cosmic ray pressure P_{CR}, turbulent pressure P, velocity dispersion c_0, and total gas+star density $\rho_{0\mathrm{T}}$ in the gas layer. We also write $\mu_0 = R\rho_0 H$. With these substitutions,

$$\frac{c^2}{G\mu_0} = \frac{\kappa(2\pi)^{1/2} c/c_0}{T_0[(1+\alpha+\beta)\rho_0/\rho_{0\mathrm{T}}]^{1/2}}. \tag{9}$$

Typically, $(1+\alpha+\beta)\rho_0/\rho_{0\mathrm{T}} \sim 1$, so the parameter T_0 in the collapse time satisfies the equation

$$T_0 \exp\left[-0.5\left(1 + \frac{(2\pi)^{1/2}\kappa c}{T_0 c_0}\right)\right] \approx \left[\frac{(1+2\kappa)^2 - \kappa^2}{4\pi}\right]^{1/2}. \tag{10}$$

Equation (10) is solved numerically for T_0 as a function of c/c_0. Then the time for triggering cloud formation in the ring is

$$t_{\mathrm{trig}} = \frac{T_0}{(G\rho_0)^{1/2}\mathcal{M}}, \tag{11}$$

and the corresponding radius is

$$R_{\mathrm{trig}} = \frac{T_0 c}{\kappa(G\rho_0)^{1/2}}. \tag{12}$$

In physical units:

$$t_{\mathrm{trig}} = \frac{80 T_0}{n_{\mathrm{H}}^{1/2}\mathcal{M}} \quad \mathrm{Myr}, \tag{13}$$

$$R_{\mathrm{trig}} = \frac{80 T_0 c}{\kappa n_{\mathrm{H}}^{1/2}} \quad \mathrm{pc}, \tag{14}$$

for T_0 of order unity, c in km s^{-1}, and ambient hydrogen density n_{H} in cm^{-3} (considering He also in ρ_0). Note that if the gas were in the shape of a sphere instead of a ring, the time of collapse would be proportional to $\mathcal{M}^{-1/2}$ instead of $\mathcal{M}^{-1}$, and the radius of collapse would be proportional to $\mathcal{M}^{1/2}$.

The age, t_{now}, and radius, R_{now}, of the Quadrant ring are currently larger than the triggering age and radius, because the triggering happened some time ago when the clusters in the arc began forming. To explain the current radius of the arc, we have to consider how the stars moved after star formation began. We consider three cases. First, the arc continued to expand as $R \propto t^{\kappa}$ for the two expansion geometries discussed above (spherical and cylindrical respectively), which means that the cavity continued to inflate with energy from the old clusters, and the arcs also continued to accumulate gas. This gives

$$R_{\mathrm{now}} = R_{\mathrm{trig}}\left(\frac{t_{\mathrm{now}}}{t_{\mathrm{trig}}}\right)^{\kappa}. \tag{15}$$

As a second alternative, we assume that the source energy input stopped when star formation began, and that the arcs decelerated faster with the continued accumulation of gas (snowplough model). Then momentum conservation gives $R^D v =$ constant in the spherical ($D = 3$) and cylindrical ($D = 2$) energy input models, so

$$R_{\mathrm{now}}^{D+1} = R_{\mathrm{trig}}^{D+1} + (D+1) R_{\mathrm{trig}}^{D} V_{\mathrm{trig}}\left(t_{\mathrm{now}} - t_{\mathrm{trig}}\right). \tag{16}$$

A third possibility is that the arcs drifted with constant speed after they began forming stars, as if the gas dynamics were not important anymore. Then

$$R_{\mathrm{now}} = R_{\mathrm{trig}} + V_{\mathrm{trig}}\left(t_{\mathrm{now}} - t_{\mathrm{trig}}\right). \tag{17}$$

4.2 Solutions for the formation and motion of Quadrant

To solve for the shell dynamics, we need the ambient hydrogen density, n_{H}. This is obtained from the H I contours in Domgörgen, Bomans & de Boer (1995) by dividing the average H I column density far outside LMC4, $\sim 1.2 \times 10^{21}$ cm^{-2}, by an assumed disc thickness. We choose a thickness equal to 400 pc, which is slightly larger than the disc thickness in the inner Milky Way, because irregular galaxies tend to have larger thicknesses than spirals (van den Bergh 1988). The result is ~ 1 cm $^{-3}$ for the Quadrant region.

We also need the velocity dispersion in the ring, c. This is not observed, but we assume that the ambient dispersion is $c_0 = 5$ km s^{-1}, and treat the ratio c/c_0 as an adjustable parameter.

The solution for $R(t)$ is obtained by searching for the value of c/c_0 which gives $T_{\mathrm{trig}} = 14$ My, the approximate time interval between the first generation of star formation (the A supergiants, $\sim$30 Myr old) and the oldest stars in Quadrant (16 Myr from Braun et al. 1997). The exact value of this time is not important here; analogous solutions can be obtained for a range of values. To find $R(t)$, we have to consider both equations (13) and (14) for the collapse condition, and equations (15), (16), or (17) for the expansion since the time of collapse, using the present Quadrant radius, $R_{\mathrm{now}} \sim 280$ pc, and the total elapsed time $t_{\mathrm{now}} = 30$ Myr (again these values are estimates, meant only to illustrate the plausibility of the basic model until better data are available for this region).

The results for the three expansion cases with spherical and cylindrical geometries are shown in Fig. 3. The solutions are very similar, because they are tightly constrained by the collapse and total ages, and by the present-day radius of Quadrant. The time when Quadrant began forming stars is indicated by a large dot, $\sim$16 Myr ago. Time is measured backwards in this diagram, with the present time equal to zero, and the events in the past written as negative time. The stellar velocities today are the slopes of these lines at $t = 0$; they range between 5 and 10 km s^{-1}, in the southernly direction.

The values of the internal ring velocity dispersions, c, that were used to fit these solutions range between 1.0 and 1.3 km s^{-1}.

The other parameter that occurs in the wind solution is the ratio of the wind luminosity L to the ambient density, ρ_0. According to equation (21) in Weaver et al. (1977), which is appropriate for a thin shell, this ratio is given by

$$\frac{L}{\rho_0} = 3.87\frac{R^5}{t^3}. \tag{18}$$

Prior to the time of star formation in our model, this ratio was

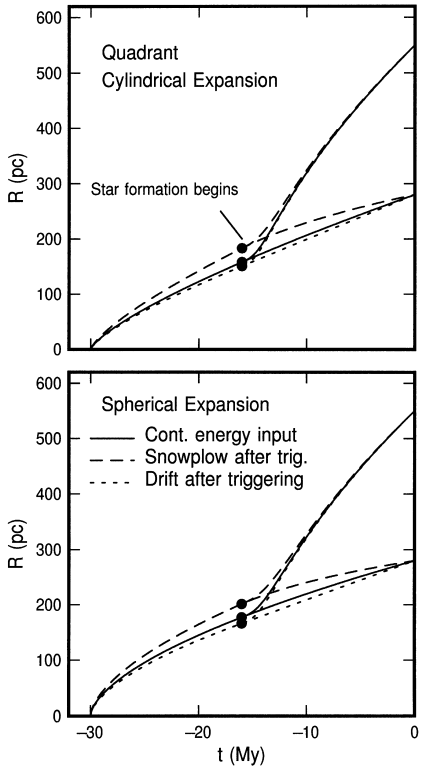

Figure 3. The radius of the proposed ring that formed the Quadrant arc is shown as a function of time for various models. The dots show the radii and times for gravitational collapse in the ring, when star formation in Quadrant is assumed to have begun.

$(2.2, 4.2, 1.6) \times 10^{60}$ erg cm^3 s^{-1} gm^{-1} for the spherical case in the post-collapse pressurized, snowplough, and constant velocity solutions respectively, and $(1.2, 2.6, 0.9) \times 10^{60}$ erg cm^3 s^{-1} gm^{-1} in the three corresponding cylindrical cases. In units of $1.3 \times 10^{36}/(1.4 m_{\rm H})$ erg cm^3 s^{-1} gm^{-1}, which is approximately the number of OB-star winds (Snow & Morton 1976) per unit external hydrogen density, these ratios are (4.0, 7.5, 2.9) and (2.2,4.7,1.8) respectively. Further multiplication by $n_{\rm H} = 1$ cm^{-3} gives the effective number of OB-star winds, which, for our assumed density and times, ranges between 2 and 8. These are typical numbers of stars with strong winds in OB associations, and not inconsistent with the six AI stars presently near the centre of the Quadrant arc.

The mass of the gas cloud that made Quadrant can be estimated from the ambient column density (1.2×10^{21} cm^{-2}), the triggering radius ($\sim 200 - 280$ pc), and the section of the circle that Quadrant represents (1/4). This mass is $(4.2 - 8.2) \times 10^5$ M$_\odot$. The total cluster mass in the arc is 3.2×10^5 M$_\odot$, based on data in Table 1 along with fig. 13 in Girardi et al. (1995). This implies that the overall efficiency for star formation was around $\sim$40–80 per cent in this triggered region. This seems high, but Quadrant is very dense with stars, and the numbers are imprecise. Also, the absence of H I gas close to Quadrant (Kim et al. 1997) suggests a high efficiency.

4.3 H I shell expansion after the Quadrant arc forms

The H I ring currently in the vicinity of Constellation III is larger than the radius of the Quadrant arc of stars. There is also recent star formation along the perimeter of this ring, and there is an unusually low density of H I in the ring centre. In our model, the H I void and the large size of the current H I ring are the result of continued expansion of the gaseous structure that originally made the Quadrant, driven in more recent times by pressure from the Quadrant stars themselves. Presumably these stars drove away the remaining gas that directly formed Quadrant, and then continued to exert a pressure on the surrounding medium, re-inflating the original cavity with hot gas from the Quadrant's stellar winds and supernovae, and making the deep H I hole in the centre of the ring. Additional pressure from supernovae in the first generation of stars would have been available too.

We can model this second generation expansion using the original equations for a wind-driven cavity (Pikelner 1968; Dyson 1973; Weaver et al. 1977), but with a solution modified to include an initial non-zero radius and velocity. These are equations (17), (18) and (19) in Weaver et al. (1977):

$$E = 2\pi R^3 P, \tag{19}$$

$$\frac{{\rm d}E}{{\rm d}t} = L - 4\pi R^2 P V, \tag{20}$$

$$\frac{\rm d}{{\rm d}t}\left(\frac{4\pi}{3} R^3 \rho_0 V\right) = 4\pi R^2 P, \tag{21}$$

for energy E, radius R, velocity V, pressure P, wind luminosity L, and ambient density ρ_0. These equations can be reduced to the single equation

$$\frac{1}{3} R^4 \frac{{\rm d}^2 V}{{\rm d}t^2} + 4R^3 V \frac{{\rm d}V}{{\rm d}t} + 5R^2 V^3 = \frac{L}{4\pi\rho_0}. \tag{22}$$

We take the initial conditions for these evolution equations to be the state of the previous generation ring at the time of star formation in Quadrant, i.e., $V = V_{\rm trig}$, and $R = R_{\rm trig}$, and we take the initial acceleration from the first generation snowplough solution, considering that the cavity pressure at the time of the Quadrant formation was much less than the new cavity pressure from the Quadrant stars. This gives the initial condition ${\rm d}V/{\rm d}t = -3V_{\rm trig}^2/R_{\rm trig}$ for 3D and $-2V_{\rm trig}^2/R_{\rm trig}$ for 2D.

The solution to this equation was determined numerically for the six cases considered above, and the resulting radii $R(t)$ for the re-inflated H I rings are shown in Fig. 3 as lines branching off from the dots and going to larger radii. We adjust the only free parameter, L/ρ_0, to give the current radius of the H I ring, which is 550 pc (again assuming a distance to the LMC of 45 kpc). Written in terms of the first-generation ratio L/ρ_0 for the same ρ_0, the second-generation ratio is larger in these solutions by the factors (156,78,220) and (286,130,368) for the spherical and cylindrical cases respectively in the pressurized, snowplough, and constant velocity solutions. Thus the Quadrant arc is more luminous than the first generation OB association by these factors of $\sim$80 to $\sim$370, considering that the average density outside the H I ring was about the same in each case. This large factor, combined with the lower age of Quadrant, explains why the pressure-driving cluster is so difficult to see in comparison to the Quadrant arc.

The current expansion speed of the H I shell in these solutions is $\sim$19 km s^{-1}, tightly constrained by the current radius and assumed age of the ring, and by the radius and age of the ring when Quadrant formed. The projected expansion speed of this H I ring is predicted to be about half of this, considering the LMC inclination (33°). This is a small enough expansion speed to be consistent with the observations (Domgörgen et al. 1995).

5 TRIGGERED STAR FORMATION IN SEXTANT

The main event in this region of the LMC is the expansion of the

giant H I ring that made Quadrant, and the continued expansion of this ring afterwards. Many other star formation sites have also appeared in the ring, particularly at later stages when the ring is dense and strongly self-gravitating. One of these may have gone on to trigger another arc of stars in the south-west, which we call Sextant. This second arc is small enough that the spherical solution for an expanding shell is probably adequate, in which case we can use the results for gravitational collapse directly from equations (16) and (17) in Elmegreen (1994), which are

$$t_{\rm trig} = \frac{1.25}{\left(G\rho_0\mathcal{M}\right)^{1/2}} \;\; ; \;\; R_{\rm trig} = \frac{5}{3}Vt_{\rm trig} = \frac{2.1c\mathcal{M}^{1/2}}{G\rho_0}. \qquad (23)$$

A plausible model for the formation of Sextant is that it was triggered by the collapse of a small swept-up shell around a cluster that formed inside the giant expanding H I ring. Then Sextant is a third generation of star formation, and the driving cluster that made Sextant is a second generation, like Quadrant, but younger.

The oldest stars in Sextant are ∼7 Myr old, according to Table 1, and the clusters near the centre of the Sextant arc, either HS 287 or 288, are probably only 10–15 Myr old, considering that HS 287 still has an H II region. Thus Sextant could have been triggered in only ∼8 Myr (= 15 − 7 My). This means, according to equation (23), that the ambient density had to be rather large. This is to be expected if Sextant was triggered inside the dense part of the H I ring.

We can find the ratio of the external density to the internal sound speed, $n_{\rm H}/c$, for the shell that made Sextant using equations (23) and (15), with the constraints that the triggering occurred $t_{\rm trig} = 8$ Myr after the first generation formed, which was $t_{\rm now} = 15$ Myr ago, and that the current size of the shell is $R_{\rm now} = 170$ pc. These numbers are not well known, but they are good enough to illustrate the procedure. Then, combining these equations to obtain $V_{\rm trig}$, we first get $t_{\rm trig}^{2/5} = (3/5)R_{\rm now}t_{\rm now}^{-3/5}V_{\rm trig}^{-1}$ by eliminating $R_{\rm trig}$ from equation (15) and the right-hand equation (23), and then, by substituting $t_{\rm trig}$ from the left-hand equation (23), we get

$$V_{\rm trig} = \left(\frac{3R_{\rm now}}{5t_{\rm now}^{3/5}}\right)^{5/4}\left[\frac{(G\rho_0)^{1/2}}{1.25c^{1/2}}\right]^{1/2}. \qquad (24)$$

Putting this into the $\mathcal{M}$ term of the left-hand equation (23), we get

$$t_{\rm trig} = \frac{1.25^{5/4}c^{5/8}}{(G\rho_0)^{5/8}}\left(\frac{5t_{\rm now}^{3/5}}{3R_{\rm now}}\right)^{5/8}. \qquad (25)$$

For c in km s^{-1}, $R_{\rm now}$ in pc, $n_{\rm H}$ in cm^{-3}, and $t_{\rm now}$ in Myr, this is

$$t_{\rm trig} = 443\left(\frac{c}{n_{\rm H}}\right)^{5/8}\left(\frac{t_{\rm now}^{3/5}}{R_{\rm now}}\right)^{5/8} \ {\rm My}. \qquad (26)$$

Now we set $t_{\rm trig} = 8$ My, $t_{\rm now} = 15$ My, and $R_{\rm now} = 170$ pc, to get $n_{\rm H}/c \sim 18$ cm^{-3} (km s^{-1})$^{-1}$. This large value indicates how the density in the environment of Sextant was likely to be large for $c \sim 1$ km s^{-1}.

The triggering radius follows from these equations in a similar manner:

$$R_{\rm trig} = \frac{5}{3}\left(\frac{1.25c^{1/2}}{(G\rho_0)^{1/2}}\right)^{3/4}\left(\frac{3R_{\rm now}}{5t_{\rm now}^{3/5}}\right)^{5/8}, \qquad (27)$$

which may be rewritten in units of km s^{-1}, pc and Myr:

$$R_{\rm trig} = 38.7\left(\frac{c}{n_{\rm H}}\right)^{3/8}\left(\frac{R_{\rm now}}{t_{\rm now}^{3/5}}\right)^{5/8} \ {\rm pc}. \qquad (28)$$

With $t_{\rm now} = 15$ My, $R_{\rm now} = 170$ pc, and $n_{\rm H}/c \sim 18$ cm^{-3} (km s^{-1})$^{-1}$, this gives $R_{\rm trig} = 117$ pc.

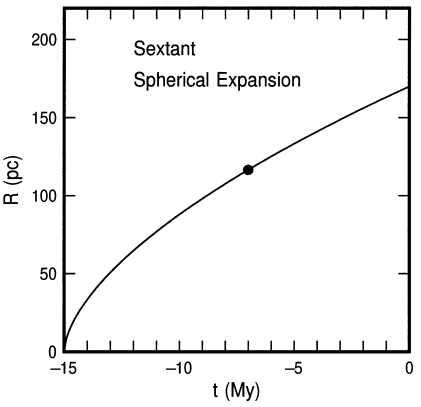

Figure 4. The radius as a function of time for the proposed shell that made the Sextant ring.

Finally, the velocity at the time of triggering becomes simply $V_{\rm trig} = (3/5)R_{\rm trig}/t_{\rm trig}$, which is ∼8.7 km s^{-1}.

Fig. 4 shows the solution $R(t)$ with the time of triggering for Sextant, using $n_{\rm H}/c \sim 18$ cm^{-3} (km s^{-1})$^{-1}$. The corresponding ratio L/ρ_0 for this shell solution is 1.4×10^{60} erg cm^3 s^{-1} gm^{-1} from equation (18), corresponding to a number of OB stars equal to ∼2.6 per unit external H I density, or to ∼48 stars if $n_{\rm H} \sim 18$ cm^{-3}. If this is too large for the clusters HS 287 and 288, then perhaps these clusters are slightly older than we assumed (making the power requirement smaller), or there was significant supernova activity in the centre of the Sextant arc, in addition to stellar winds.

6 LOW SHEAR AND LARGE DISC THICKNESS AS A PREREQUISITE FOR FORMING GIANT SHELLS AND RINGS

The large size and round shape of the LMC4 superbubble is most likely the result of low shear in this region. Otherwise, the ring resembles the Lindblad ring in the solar neighbourhood in overall dimension and mass, even to the extent that the Lindblad ring also has an old and faint dispersed OB association in the centre (Blaauw 1984), with significant star formation along the periphery (Pöppel 1997). The low shear in the LMC makes the LMC4 region morphologically different than the Lindblad ring, however.

The rotation speed in the LMC at the radius of LMC4, $R \sim 2.6$ kpc, is about $V \sim 55$ km s^{-1} deprojected, and it is in a flat part of the rotation curve (Luks & Rohlfs 1992). Thus the shear time, which is the inverse of the Oort A parameter, is $A^{-1} \sim 2R/V \sim 94$ My. This is ∼3 times larger than the age of the H I ring according to our model (∼30 My), and so the ring is still nearly circular. Generally, the pitch angle i of an initially circular feature that shears with time t is given by $\tan i = -tR{\rm d}\Omega/{\rm d}R$ for angular rate $\Omega = V/R$. For the LMC4 region after $t = 30$ My, this pitch angle is 58°, which is sufficiently close to the radial direction (90°) that the ring hardly looks swept back, especially with the ∼33° inclination of the galaxy.

Shear is generally low in other dwarf galaxies too, such as HoII, where other giant rings have been found (Puche et al. 1992). These rings can be many tens of millions of years old and still nearly circular. At such large ages, the central clusters may be dispersed over regions several hundred parsecs in diameter. The only obvious tracers of these first generation stars would be supergiants and Cepheids, as in the central region of LMC4. The stars may even disperse from their clusters faster than the average speed of the ring

at very late times, after the ring has stalled (i.e., > 50 My). Then the brightest stars from all of the neighbouring expansion regions can mix together, smoothing out the initial associations. The main-sequence stars that formed in these associations will blend with the older stars in the disc.

Kiloparsec-size rings can also occur in giant galaxies, but primarily in the outer spiral arms, where the shear and flow-through times are very large. Shear is generally low inside spiral arms because of angular momentum conservation in the gas during the spiral wave compression (Elmegreen 1992). In the outer regions, particularly near corotation or beyond, the flow-through time can exceed 100 My. Then star-forming regions can inflate giant shells for several generations. Examples of this might be the giant shells in the southern spiral arm of M83 (Sandage & Bedke 1988), and in the northern spiral arm of M51 (see the 15μ-B image in Block et al. 1997).

A second condition for the formation of giant shells and rings is that the disc thickness has to exceed the perturbation diameter of the high-pressure region, or else the high-pressure gas will escape into the halo (MacLow & McCray 1988; Tenorio-Tagle, Rozyczka & Bodenheimer 1990). Such large disc thicknesses are generally believed to be appropriate for dwarf galaxies like the LMC (Hodge & Hitchcock 1966; van den Bergh 1988; Puche et al. 1992) and for the outer regions of giant spiral galaxies, because of the low surface brightnesses, and therefore low stellar surface densities, of the underlying discs. With a low surface mass density in a disc, the $\sim$5 km s^{-1} turbulent motions of the gas bring it to a large scaleheight, which scales inversely with the total surface density inside the gas layer. Rings can become even larger than the disc thickness after the interior pressure decreases, simply by momentum conservation from their motion in the plane. For example, if the shell speed at the time of breakout is twice the external velocity dispersion, then the final ring diameter will be $2^{1/2}$ times the disc thickness by the time the expansion has slowed to the external dispersion; i.e., it will have picked up twice the mass in that final stage, and therefore slow to half the speed.

In view of the low shear and large likely disc thickness in the outer part of the LMC, it is not surprising that several supergiant rings occur there, and that these rings today have only faint remnants of the powerful stars that once created them.

7 CONCLUSIONS

Two arcs of star clusters inside and on the rim of the superbubble LMC4, including what is commonly referred to as Constellation III, may have been formed by the self-gravitational collapse of gas in swept-up pieces of rings or shells. The dimensions and time sequences for these triggerings are reasonable, as is the energetics. This triggering model differs qualitatively from others in which pre-existing clouds are squeezed into star formation by passing shock fronts. The regular form of the Quadrant and Sextant arcs resembles more a piece of a ring or shell than a random arrangement of pre-existing clouds.

The conditions in the outer part of the LMC and other dwarf galaxies, and in the outer spiral arms of giant spiral galaxies, are favourable for the formation of giant gas shells and rings in which the first generation of stars is so old and dispersed that it is barely visible anymore. All that is required for this is a low rate of shear and a relatively large disc thickness.

A recent study suggests that gamma-ray bursts from old star-forming regions might also play a role in enlarging supernova cavities beyond the size of the disc thickness (Efremov, Elmegreen & Hodge 1998). This would not affect the general triggering scenario discussed here, but it would affect the estimate for the number of stars that led to either the first or the second generation pressures.

ACKNOWLEDGMENTS

We are grateful to the referee for valuable suggestions, and to P. Bogdanovsky, whose computer program helped in searches for triggering stars. Dr K. Olsen kindly provided a tiff image for the star field in Fig. 1.

REFERENCES

Berdnikov L. N., Vozyakova O. V., Dambis A. K., 1996, Pis'ma Astron. Zh., 22, 935
Bertelli G., Bressan A., Fagotto F., Nasi E., 1994, A&AS, 106, 275
Bica E., Claria J. J., Dottori H., Santos J. F. C., Piatti A. E., 1996, ApJS, 102, 57
Blaauw A., 1984, Ir. Astron. J., 16, 141
Block D. L., Elmegreen B. G., Stockton A., Sauvage M., 1997, ApJ, 486, L95
Boss A. P., 1995, ApJ, 439, 224
Braun J. M., Bomans D. J., Will J.-M., de Boer K. S., 1997, A&A, 328, 167
Castor J., McCray R., Weaver R., 1975, ApJ, 200, L107
Comerón F., Torra J., Gómez A. E., 1998, A&A, 330, 975
de Boer K. S., Braun J. M., Vallenari A., Mebold U., 1998, A&A, 329, L49
Dibai E. A., 1958, Sov. Astron. AJ, 2, 429
Domgörgen H., Bomans D. J., de Boer K. S., 1995, A&A, 296, 523
Dopita M. A., Mathewson D. S., Ford V. L., 1985, ApJ, 297, 599
Dyson J. E., 1968, Ap&SS, 1, 338
Dyson J. E., 1973, A&A, 23, 381
Efremov Yu. N., 1997, Astron. Rep., 41, 325
Efremov Yu. N., Elmegreen B. G., 1998, MNRAS, 299, 588
Efremov Yu. N., Schilbach E., Zinnecker H., 1997, Astron. Nachr., 318, 335
Efremov Yu. N., Elmegreen B. G., Hodge P. W., 1998, ApJ, 501, 163
Ehlerová S., Palous J., Theis Ch., Hensler G., 1997, A&A, 328, 121
Elmegreen B. G., 1982a, in Brahic A., ed., The Formation of Planetary Systems. Cepadues Editions, Toulouse, p. 61
Elmegreen B. G., 1982b, in Beckman J., Phillips J., eds, Submillimetre-Wave Astronomy. Cambridge Univ. Press, Cambridge, p. 1
Elmegreen B. G., 1985, in Lucas A., Omont A., Stora R., eds, Primary and Secondary Mechanisms of Giant Cloud Formation in Birth and Infancy of Stars. Elsevier Science Publishers B. V., Amsterdam, p. 215
Elmegreen B. G., 1992, in Pfenniger D., Bartholdi P., eds, Interstellar Gas Dynamics. Springer-Verlag, Berlin, p. 157
Elmegreen B. G., 1994, ApJ, 427, 384
Elmegreen B. G., 1998, in Woodward C. E., Thronson H. A., Shull M., eds, ASP Conf. Ser. Vol. 148, Origins of Galaxies, Stars, Planets and Life. Astron. Soc. Pac., San Francisco, p. 149
Elmegreen B. G., Lada Ch. J., 1977, ApJ, 214, 725
Fernley J., Barnes T. G., Skillen I., Hawley S. L., Hanley C. J., Evans D. W., Solano E., Garrido R., 1998, A&A, 330, 515
Girardi L., Chiosi C., Bertelli G., Bressan A., 1995, A&A, 298, 87
Hodge P. W., 1967, PASP, 79, 29
Hodge P. W., Hitchcock J. L., 1966, PASP, 78, 79
Hodge P. W., Wright F. W., 1967, The Large Magellanic Cloud. Smithsonian Press, Washington
Kim S., Staveley-Smith L., Sault R. J., Kesteven M. J., McConnell D., Freeman K. C., 1997, Proc. Astron. Soc. Aust., 14, 119
Lefloch B., Lazareff B., 1994, A&A, 289, 559
Lucke P. B., Hodge P. W., 1970, AJ, 75, 171
Luks Th., Rohlfs K., 1992, A&A, 263, 41
MacLow M.-M., McCray R., 1988, ApJ, 324, 776
McCray R., Kafatos M., 1987, ApJ, 317, 190
McGee R. X., Milton J. A., 1966, Aust. J. Phys., 19, 343

McKibben Nail V., Shapley H., 1953, Harvard Rep. 373
Meaburn J., 1980, MNRAS, 192, 365
Meaburn J., Terret D. L., 1980, A&A, 89, 126
Olsen K. A. G., Hodge P. W., Wilcots E. M., Pastwick L., 1997, ApJ, 475, 545
Ostriker J. P., Cowie L. L., 1981, ApJ, 243, L127
Petr M., 1994, PhD dissertation, Univ. Bonn, Germany
Pikelner S. B., 1968, Astrophys. Lett., 2, 97
Pöppel W., 1997, Fundam. Cosmic Phys., 18, 1
Puche D., Westpfahl D., Brinks E., Roy J-R., 1992, AJ, 103, 1841
Rebeirot E., Martin N., Prevot L., Robin A., Peyrin Y., Maines P., Rousseau J., 1983, A&AS, 51, 277
Reid N., Mould J., Thompson I., 1987, ApJ, 323, 433
Rousseau E., Martin N., Prevot L. Robin A., Brunet J. P., 1978, Ap&SS, 31, 243
Sandage A., Bedke J., 1988, Atlas of Galaxies Useful for Measuring the Cosmological Distance Scale. NASA, Washington D.C.
Shklovsky I. S., 1960, Soviet Astron. AJ, 4, 355
Snow T. P., Jr., Morton D. C., 1976, ApJS, 32, 429
Tenorio-Tagle G., 1981, A&A, 94, 338
Tenorio-Tagle G., Bodenheimer P., 1988, ARA&A, 26, 146
Tenorio-Tagle G., Rozyczka M. & Bodenheimer P., 1990, A&A, 237, 207
Theis Ch., Ehlerová S., Palous J., Hensler G., 1997, in Breitschwerdt D., Freyberg M., eds, Proc. IAU Colloq. 166, The Local Bubble and Beyond. Springer, Berlin, p. 409
Vader P., Chaboyer B., 1995, ApJ, 445, 691
van den Bergh S., 1981, A&AS, 46, 79
van den Bergh S., 1988, PASP, 100, 344
Vishniac E. T., 1983, ApJ, 274, 152
Weaver R., McCray R., Castor J., Shapiro P., Moore R., 1977, ApJ, 218, 377
Westerlund B. E., Mathewson D. S., 1966, MNRAS, 131, 371

This paper has been typeset from a TEX/LATEX file prepared by the author.